JOURNAL OF Materials CHEMISTRY

Study on the structural and electrical properties of the double perovskite oxide $SrMn_{0.5}Nb_{0.5}O_{3-\delta}$

Shanwen Tao and John T. S. Irvine*

School of Chemistry, University of St Andrews, Fife, Scotland, UK KY16 9ST. E-mail: jtsi@st-andrews.ac.uk

Received 29th October 2001, Accepted 1st May 2002
First published as an Advance Article on the web 7th June 2002

The new non-stoichiometric mixed perovskite $SrMn_{0.5}Nb_{0.5}O_{3-\delta}$ has a cubic double perovskite structure similar to that of Sr_2CrNbO_6 with space group $Fm\bar{3}m$ (225), $a = 7.9338(3)$ Å, $V = 499.39(6)$ Å^3 according to X-ray diffraction. The material is redox stable and maintains its structure in a reducing atmosphere. After reducing in 5% H_2 at 900 °C for 6 hours, $SrMn_{0.5}Nb_{0.5}O_{3-\delta}$ still exhibits a cubic structure with space group $Pm\bar{3}m$ (221), $a = 4.0022(5)$ Å, $V = 64.10(8)$ Å^3. A lattice volume expansion of 2.7% was observed during the reduction. TGA analysis indicates $SrMn_{0.5}Nb_{0.5}O_{3-\delta}$ loses 0.125 oxygen per formula unit from 500 to 950 °C in 5% H_2. This weight change is consistent with a reduction from $SrMn_{0.5}Nb_{0.5}O_3$ to $SrMn_{0.5}Nb_{0.5}O_{2.875}$. The morphology of this material does not significantly change on reduction according to SEM observation. A.c. impedance measurements indicate that electronic conduction is probably dominant both in air and 5% H_2. The conductivities of this material in air, humidified 5% H_2 and 5% H_2 were 1.23, 6.4×10^{-2} and 3.1×10^{-2} S cm^{-1} respectively at 900 °C. The decrease of d.c. conductivity of $SrMn_{0.5}Nb_{0.5}O_{3-\delta}$ at p_{O_2} below 10^{-12} atm indicates p-type electronic conduction. The higher apparent conduction activation energy and lower conductivity in H_2 than in air may be due to the contribution of lattice expansion which results in poorer overlap of both σ and π bonds, which makes the hopping of electron holes more difficult. The d.c. conductivity of $SrMn_{0.5}Nb_{0.5}O_{3-\delta}$ at low p_{O_2} exhibits a $p_{O_2}^{1/6}$ dependence that is interpreted by a simple defect chemistry model.

1. Introduction

Mixed ionic–electronic conductors (MIECs) which exhibit both electronic and ionic conductivity have numerous technological applications such as electrodes for solid oxide fuel cells (SOFCs), gas semi-permeation membranes, water electrolysis and electrocatalytic reactions.[1–5] It has been reported that some non-stoichiometric mixed perovskites with formula $A_3B'_{1+x}B''_{2-x}O_{9-\delta}$ where A is an alkali earth element Ca, Sr, Ba *etc*., B′ is an element with valence +2 or +3 and B″ is an element with valence +5, such as Nb and Ta, exhibit quite high proton and oxygen-ion conductivity.[6–11] It is expected that mixed ionic and electronic conductors may be found in these compounds if the B-sites are partially substituted by appropriate first row transition elements. Such mixed conductors may provide potential anode materials for fuel cell applications. The requirements for SOFC anode materials are good chemical and mechanical stability under SOFC operating conditions, high ionic (O^{2-} or H^+) and electronic conductivity over a wide range of p_{O_2} and good chemical and thermal compatibility with electrolyte and interconnect materials. The conductivity and stability should be investigated first when exploring new materials for such applications. First row transition elements from group VIII or below are chemically stable in a reducing atmosphere at high temperature, which are SOFC anode conditions. Manganese is of particular interest because Mn promotes electrochemical reaction as an electrocatalyst coated on YSZ electrolyte and reduces overpotential.[12] As reported by Glockner *et al*.,[10] $Sr_3Sr_{1.5}Nb_{1.5}O_{9-\delta}$ exhibits quite high ionic conductivity at elevated temperature. It is expected that some mixed conductors may be obtained if strontium at B-sites is replaced by manganese. Therefore, in this paper, we report the structure, stability and electrical properties of a new perovskite oxide $SrMn_{0.5}Nb_{0.5}O_{3-\delta}$. It is a partially ordered double perovskite oxide in air and a primitive perovskite in 5% H_2 according to XRD analysis. For convenience, the formula of the sample in both atmospheres is written as $SrMn_{0.5}Nb_{0.5}O_{3-\delta}$ from the chemical composition, disregarding the structure aspects.

2. Experimental

$SrMn_{0.5}Nb_{0.5}O_{3-\delta}$ was synthesised by solid state reaction using $SrCO_3$, MnO_2 and Nb_2O_5 as starting materials. $SrCO_3$ and MnO_2 were dried at 100–300 °C, Nb_2O_5 at 500 °C overnight to remove absorbed H_2O and CO_2. Stoichiometric amounts were mixed and ball milled in zirconia containers with zirconia balls for two 15 minute periods. The final firing temperature was 1400 °C with intermediate grindings until a single phase was obtained. To study the phase stability of the material in reducing atmospheres, the sample obtained at 1400 °C was further heated at 900 °C for 6 hours and cooled down to room temperature in 5%H_2.

XRD analyses of powders reacted at different temperatures were carried out on a Stoe Stadi-P diffractometer to determine phase purity and measure crystal parameters. Structure refinement was performed by the Rietveld method using the program General Structure Analysis System (GSAS).[13] Thermal analysis of $SrMn_{0.5}Nb_{0.5}O_{3-\delta}$ was carried out on a Rheometric Scientific TG 1000 M Plus, and a TA Instruments SDT2960 from room temperature to 950 °C (5 °C min^{-1}), holding at 950 °C for 30 minutes then cooling down to 30 °C (10 °C min^{-1}) under flowing 5% H_2 in argon at a rate of 35 ml min^{-1}. SEM observations were carried out on a JEOL 5600 scanning electron microscopy.

For a.c. impedance measurements in air, a Schlumberger Solartron 1260 Frequency Response Analyser coupled with a 1287 Electrochemical Interface controlled by Zplot electrochemical impedance software was used over the frequency range 1 MHz to 100 mHz. A.c. impedance measurements were made in 50 °C steps in air between 600 and 900 °C. The d.c.

 DOI: 10.1039/b204248g

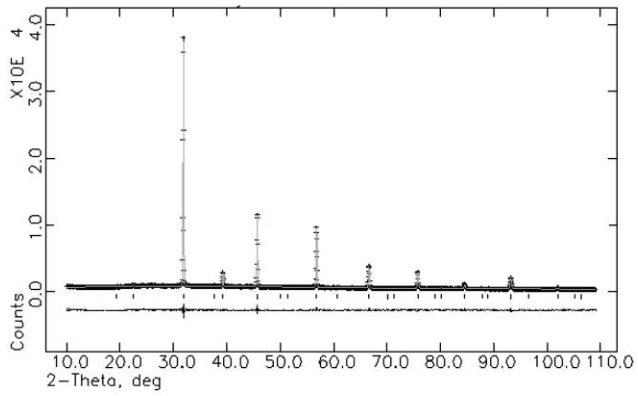

Fig. 1 X-Ray diffraction profiles of $SrMn_{0.5}Nb_{0.5}O_{3-\delta}$ formed at 1400 °C, showing observed pattern, peak positions and difference profile for $Fm\bar{3}m$, $a = 7.9338(3)$ Å.

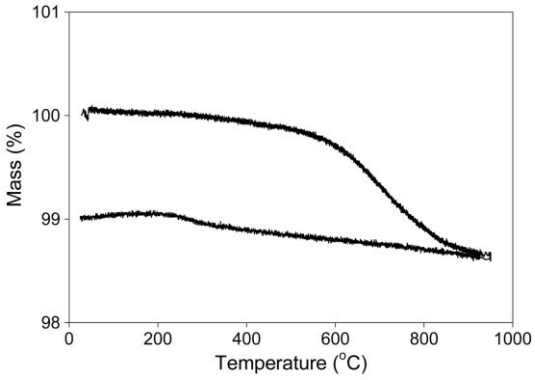

Fig. 2 TGA analysis of $SrMn_{0.5}Nb_{0.5}O_{3-\delta}$ in 5%H_2, heated at 10 °C min^{-1} to 950 °C and then cooled at 10 °C min^{-1}.

conductivity was measured by a conventional four-terminal method using a Keithley 220 Programmable Current Source to control current and a Schlumberger Solartron 7150 Digital Multimeter to measure the voltage. The $SrMn_{0.5}Nb_{0.5}O_{3-\delta}$ samples were mounted with four Pt wire electrodes to measure the d.c. conductivity dependence upon p_{O_2} in a slowly varying atmosphere, which was monitored by a zirconia oxygen sensor. The conductivity in air was measured by the four-terminal d.c. method and in wet and normal 5% H_2 by a.c. impedance. The wet hydrogen was supplied by bubbling 5% H_2/95% Ar through room temperature water. The composition of wet hydrogen is approximately 4.9% H_2, 2.3% H_2O and 92.8% Ar.

3. Results and discussion

The new phase, $SrMn_{0.5}Nb_{0.5}O_{3-\delta}$ was obtained on reaction of the carbonate and oxide precursors. The final firing conditions were 1400 °C for 12 hours. The phase is basically pure except for a very weak peak with relative intensity 0.6% at $2\theta \approx 36.17°$ or ($d \approx 2.48$ Å). Possible matches are the strongest (211) peak of Mn_3O_4 (JCPDS No. 24-734) or the (021) peak of MnO (JCPDS No. 4-326), both possible stable forms of un-reacted manganese oxide at elevated temperatures.[14] After further heating and grindings, a single perovskite phase was obtained. Fig. 1 shows the X-ray diffraction patterns of $SrMn_{0.5}Nb_{0.5}O_{3-\delta}$ obtained at 1400 °C. Its pattern looks like a typical primitive perovskite oxide; however, the appearance of a weak peak at $2\theta \sim 37.6°$ indicating that some extent of B-site ordering may happen in the structure as in the case of Sr_2CrNbO_6.[15] Therefore, space group $Fm\bar{3}m$ (225) was chosen for Rietveld refinement using the GSAS program suite.[13] The two B-sites are shared by both manganese and niobium with Mn-rich 4a sites and Nb-rich 4b sites (Table 1). Refinement of the oxygen site occupancy was not very conclusive due to the insensitivity of powder X-ray diffraction to small variations in oxygen content in the presence of higher atomic number elements although the refinements were consistent with full occupation of these sites. The oxygen occupancy at the 24e sites was fixed at 1 during the refinement as the initial stoichiometry seems most likely to be $SrMn_{0.5}Nb_{0.5}O_3$, as discussed below. The thermal factors of manganese and niobium, which share the same B-site, were constrained to be equal. After the refinement, reasonable thermal factors, *R*-values and good pattern fit were obtained indicating that it is a reasonable model. The observed, calculated and difference profiles for the refinement of $SrMn_{0.5}Nb_{0.5}O_{3-\delta}$ are shown in Fig. 1. The final refined structure data are given in Table 1.

Table 1 Structure parameters of $SrMn_{0.5}Nb_{0.5}O_3$ prepared at 1400 °C from X-ray diffraction data

Atom	Site	Occupancy	*x*	*y*	*z*	U_{iso} (Å^2)
Sr	8c	1	0.25	0.25	0.25	0.0256(7)
Mn	4a	0.66(1)	0	0	0	0.0200(3)
Nb	4a	0.34(1)	0	0	0	0.0200(3)
Mn	4b	0.34(1)	0.5	0.5	0.5	0.0342(2)
Nb	4b	0.66(1)	0.5	0.5	0.5	0.0342(2)
O	24e	1	0.2355(8)	0	0	0.0447(17)

Note. Space group $Fm\bar{3}m$ (225); $a = 7.9338(3)$ Å, $V = 499.39(6)$ Å^3. $R_{wp} = 5.25\%$, $R_p = 4.93\%$, $\chi_{red}^2 = 3.074$.

Fig. 2 shows the thermogravimetric analyses (TGA) of $SrMn_{0.5}Nb_{0.5}O_{3-\delta}$ performed in dry 5% H_2. The as-prepared $SrMn_{0.5}Nb_{0.5}O_{3-\delta}$ started to lose mass at around 500 °C. The total weight loss is 1.02 wt% between 500 and 950 °C which is lower than the calculated weight loss 1.91 wt%. from Mn^{III} to Mn^{II}. It is believed that manganese cannot be totally reduced to Mn^{II} under these conditions because the conductivity of $SrMn_{0.5}Nb_{0.5}O_{3-\delta}$ in 5% H_2 (as shown later in Fig. 5) is significantly higher than expected for having Mn^{II} and Nb^{V} at B-sites (see later). It is uncertain whether Mn exhibits the oxidation state of +3 in the sample obtained in air. It is most likely that the manganese oxidation state is a mixture of +2 and +3 in 5% H_2. It must also be assumed that niobium maintains its +5 valence, as anticipated from TGA analysis of pure Nb_2O_5, no significant mass change due to the reduction of niobium was observed. Density measurements were using standard pycnometric techniques. The obtained density was 5.63(5) g cm^{-3} compared to the theoretical values of 5.572 g cm^{-3} for $SrMn_{0.5}Nb_{0.5}O_3$ and 5.519 g cm^{-3} for $SrMn_{0.5}Nb_{0.5}O_{2.875}$. This value clearly indicates that the composition before reduction is $SrMn_{0.5}Nb_{0.5}O_3$ as any oxygen vacancies, or indeed cation vacancies, will reduce density even further below the observed value. It is assumed that interstitials are not present in this perovskite lattice. The slight weight gain for $SrMn_{0.5}Nb_{0.5}O_{3-\delta}$ during cooling may be attributed to the reoxidation of the sample, although it could easily be drift due to buoyancy effects.

TGA itself cannot directly determine the phase stability of materials at high temperatures in the case of phase segregation. In order to further determine the chemical stability of $SrMn_{0.5}Nb_{0.5}O_{3-\delta}$ in a reducing atmosphere, the as-prepared $SrMn_{0.5}Nb_{0.5}O_{3-\delta}$ obtained in air was reduced in 5% H_2/95% Ar for 6 hours and cooled down to room temperature under 5% H_2. XRD analysis indicates that the reduced $SrMn_{0.5}Nb_{0.5}O_{3-\delta}$ is a single phase with a cubic structure indicating that $SrMn_{0.5}Nb_{0.5}O_{3-\delta}$ is stable in 5% H_2 at 900 °C. A close profile fit was achieved when the same model $Pm\bar{3}m$ (221) was used for Rietveld refinement (Fig. 3). The same strategy as for the unreduced sample was applied during the refinement. Table 2 lists the final refined structure data. It was found that the lattice parameter *a* for the primitive perovskite unit increased from 3.9681(2) to 4.0022(5) Å. The cell volume expands 2.7% during the reduction, which may be attributed to the reduction of

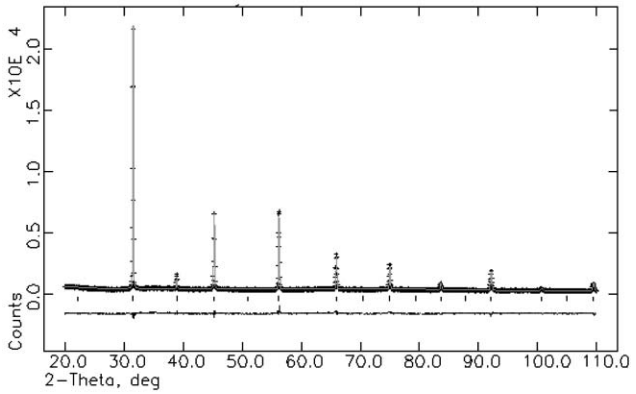

Fig. 3 X-Ray diffraction profiles of $SrMn_{0.5}Nb_{0.5}O_{3-\delta}$ after heating at 900 °C in 5% H_2 for 6 hours, showing observed pattern, peak positions and difference profile for $Pm\bar{3}m$, $a = 4.0022(5)$ Å.

Table 2 Structure parameters of $SrMn_{0.5}Nb_{0.5}O_{2.875}$ after firing at 900 °C in 5% H_2 for 6 hours from X-ray diffraction data

Atom	Site	Occupancy	x	y	z	U_{iso}/Å^2
Sr	1a	1	0	0	0	0.0238(9)
Mn	1b	0.5	0.5	0.5	0.5	0.0141(9)
Nb	1b	0.5	0.5	0.5	0.5	0.0141(9)
O	3c	0.9583	0	0.5	0.5	0.0277(17)

Note. Space group $Pm\bar{3}m$ (221); $a = 4.0022(5)$ Å, $V = 64.10(8)$ Å^3. $R_{wp} = 5.71\%$, $R_p = 5.27\%$, $\chi_{red}^2 = 2.768$.

manganese. The ionic sizes of Mn^{3+} and Mn^{2+} are 0.65 and 0.82 Å, respectively, assuming a high spin configuration for octahedrally coordinated Mn in the B-sites environment in a primitive perovskite.[16] The oxygen site occupancy again refined too close to 1 and so was set to 0.9583 corresponding to $SrMn^{II}_{0.25}Mn^{III}_{0.25}Nb^{V}_{0.5}O_{2.875}$ as indicated by density and TG measurements.

The SEM pictures of the powders before and after the reduction are shown in Fig. 4. The sample is quite homogeneous with secondary particle size 5–10 μm (Fig. 4a). However, after the

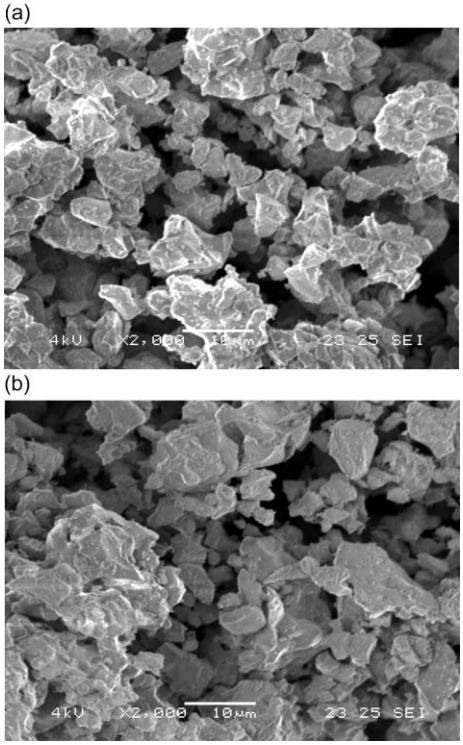

Fig. 4 SEM pictures of $SrMn_{0.5}Nb_{0.5}O_{3-\delta}$ formed at 1400 °C (a) and after further heating at 900 °C in 5% H_2 for 6 hours (b).

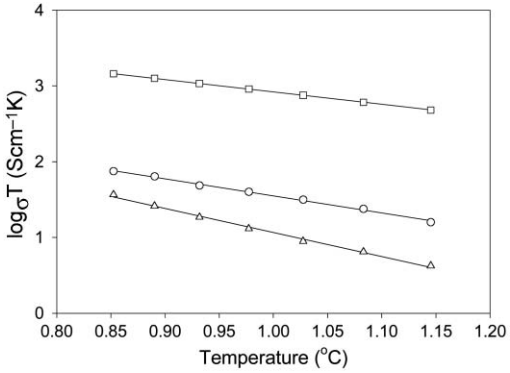

Fig. 5 The conductivity of $SrMn_{0.5}Nb_{0.5}O_{3-\delta}$ in air (□) measured by 4-terminal d.c. methods and, in wet 5%H_2 (○) and 5% H_2 (Δ) measured by a.c. impedance.

reduction, the sample becomes less homogeneous and particle agglomeration was observed (Fig. 4b) although it is insignificant.

Besides the stability, the electrical properties are very important for an electrode material. The conductivity of $SrMn_{0.5}Nb_{0.5}O_{3-\delta}$ in air was measured by a 4-terminal d.c. method because the conductivity is too high for the two-terminal a.c. impedance technique. The conductivities in 5% H_2 and humidified 5% H_2 were measured by a.c. impedance. The humidified 5% H_2 was supplied by 5% H_2 bubbling through room temperature water. The total conductivities of $SrMn_{0.5}Nb_{0.5}O_{3-\delta}$ in air, humidified and un-humidified 5% H_2 of the material were measured as 1.23, 6.4×10^{-2} and 3.1×10^{-2} S cm^{-1} respectively at 900 °C (Fig. 5). In all three atmospheres, no low frequency arc was observed in the impedance spectra obtained in air and wet hydrogen that would indicate diffusion or charge transfer limitation, demonstrating that electronic conduction is more important than ionic. At most temperatures and under most conditions only a single intercept was observed in the impedance spectra. In dry 5% H_2, the grain boundary arc was observed at 300 °C, but the contribution to the total resistance of ground boundary resistance was only about 16%. This indicated that the bulk resistance is dominant at higher temperatures as the grain boundary component was observed to have a larger thermal activation energy. The apparent grain conduction activation energies between 600 ~ 900°C are 0.32 ± 0.01, 0.45 ± 0.03 and 0.63 ± 0.04 eV in air, humidified and un-humidified 5% H_2, respectively. Those with higher oxidation states exhibit higher conductivity and lower conduction activation energy. Similar phenomena were observed by Kruth and West[17] in $Ca_2Mn_{2-x}Nb_xO_\gamma$ perovskites.

The high electronic conductivity of $SrMn_{0.5}Nb_{0.5}O_{3-\delta}$ may involve the 3d orbitals. Assuming manganese is in a high spin state and neglecting any Jahn–Teller splitting, then the energy level configurations for manganese ions are: $Mn^{2+}: t_{2g}^3e_g^2$; $Mn^{3+}: t_{2g}^3e_g^1$. As illustrated by Tuller,[18] in perovskite, the $3e_g$ orbital of B-site cations, *e.g.* Mn^{n+}, may overlap with the nearby $2p_\sigma$ orbital from the split O_{2p} to form σ-bonds (e_g-p_σ-e_g bond), meanwhile, the $3t_{2g}$ orbital of manganese ions may overlap with the $2p_\pi$ of O^{2-} ions to form weaker π-bonds (t_{2g}-p_π-t_{2g} bond). The third possibility of Mn d-orbital interactions may be the direct t_{2g}-t_{2g} overlap, as is the case in TiO,[19] which is unlikely because of the large Mn–Mn distance across the face diagonal. It is supposed that electrons (e′) or electron holes (h•) may hop from one Mn ion through the σ or π-bonds to a nearby Mn ion resulting in electronic conduction. The electronic conduction may relate to the e_g electron structure if the σ bonds are the bridge. $SrMn_{0.5}Nb_{0.5}O_{3-\delta}$ should be an insulator if the Mn valence is +2 because the hole concentration is very low.

$$0 = h^\bullet + e'$$

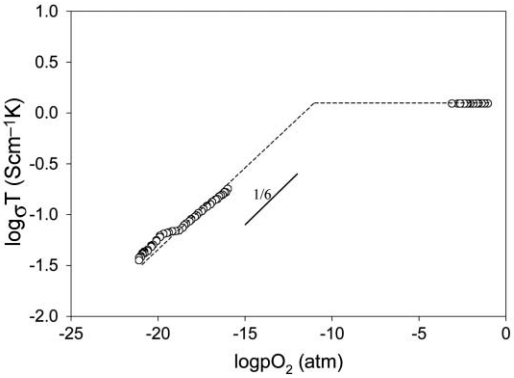

Fig. 6 Isothermal conductivity *vs.* p_{O_2} diagram for $SrMn_{0.5}Nb_{0.5}O_{3-\delta}$ starting at 900 °C. Data shown are those obtained close to fixed point p_{O_2} values in dry 5% H_2, wet 5% H_2, dry Ar and air. Thus only data that are close to equilibrium are presented. The dotted line illustrates the expected response outwith these regions.

On the other hand, if the Mn is in oxidation state +3 it may be a good conductor because the e_g orbital is not fully occupied. From this point of view, the conductivity of $SrMn_{0.5}Nb_{0.5}O_{3-\delta}$ in air should be higher than that in H_2, which is consistent with our data. If the electron transfer is through the π-bonds, the electron conductivity of $SrMn_{0.5}Nb_{0.5}O_{3-\delta}$ should not be affected by the change of manganese e_g electron structure because the t_{2g} orbital is unchanged. It is hard to say whether this is the possible conduction path of $SrMn_{0.5}Nb_{0.5}O_{3-\delta}$ because, in considering the lattice expansion as described above, the conductivity decrease in reducing atmospheres may also be attributed to the lower degree of overlap of both σ and π bonds. The Mn–O distance becomes larger, which makes the hopping of electron holes more difficult resulting in higher conduction activation energy and lower conductivity in H_2 than in air. The tilting of the BO_6 octahedra is not a factor because the Mn–O–Mn bond angles in $SrMn_{0.5}Nb_{0.5}O_{3-\delta}$ are supposed 180° with a symmetry $Pm\bar{3}m$. Another consideration which may influence the electronic and ionic conductivities is the concentration of oxygen vacancies. The electrons for reduction of manganese come from loss of lattice oxygen and creation of oxygen vacancies.

$$O_O^{\times} = V_O^{\bullet\bullet} + \tfrac{1}{2}O_2(g) + 2e'$$

The yielded O_2 gas may react with H_2 to form water while created electrons may be trapped by manganese. With increasing oxygen deficiency, the 3D hopping path for electrons or holes through Mn–O–Mn close contacts might be affected because some are blocked by oxygen vacancies leading to lower electron conductivity which is consistent with the observed conductivity as shown in Fig. 5 and Fig. 6. With increase of charge carriers $V_O^{\bullet\bullet}$, the oxygen ion conductivity may increase if the formation of defect clusters and ordering of oxygen vacancies are negligible.

As shown in Fig. 6, for p_{O_2} values below 10^{-12} atm, the conductivity decreases with decreasing p_{O_2} indicating that the material exhibits p-type conduction. The log σ *vs.* log p_{O_2} dependence of p-type electronic conductivity at low p_{O_2} gives a slope 1/6, in accord with the value expected for standard defect p-type conductivity associated with oxygen uptake on increasing p_{O_2}.

4. Conclusions

The new non-stoichiometric mixed perovskite $SrMn_{0.5}Nb_{0.5}O_{3-\delta}$ was synthesised by solid state reaction. It exhibits a cubic structure with space group $Fm\bar{3}m$ (225), $a = 7.9338(3)$ Å, $V = 499.39(6)$ Å^3 according to X-ray diffraction. The perovskite structure is retained in 5% H_2 until at least 900 °C. In a reducing atmosphere, it maintains the cubic structure and a lattice expansion was observed. The reduced sample has a cubic structure with space group $Pm\bar{3}m$ (221), $a = 4.0022(5)$ Å, $V = 64.10(8)$ Å^3. TGA and density measurements indicate that in air/oxygen the stoichiometry is essentially $SrMn^{III}_{0.5}Nb^{V}_{0.5}O_3$ and on reduction heating to 900 °C in 5% H_2 is $SrMn^{II}_{-0.25}Mn^{III}_{0.25}Nb^{V}_{0.5}O_{2.875}$, these compositions are consistent with refined XRD structure data. The morphology of this material does not significantly change on reduction according to SEM observation. A.c. impedance measurements indicate that electronic conduction is likely to be dominant. The conductivities of this material in air, humidified 5% H_2 and 5% H_2 were 1.23, 6.4×10^{-2} and 3.1×10^{-2} S cm^{-1} respectively at 900 °C. The decrease of d.c. conductivity of $SrMn_{0.5}Nb_{0.5}O_{3-\delta}$ at p_{O_2} below 10^{-12} atm indicates a p-type electronic conduction. The variation of conductivity and conduction activation energy of $SrMn_{0.5}Nb_{0.5}O_{3-\delta}$ in different atmospheres may be discussed in several ways. The electron holes may hop through the Mn–O e_g-p_σ-e_g σ-bonds and/or t_{2g}-p_π-t_{2g} π-bonds. The higher apparent conduction activation energy and lower conductivity in H_2 than in air may be due to the contribution of lattice expansion, which results in a lower degree of overlap of both σ and π bonds, which makes the hopping of electrons and electron holes more difficult. The increasing oxygen deficiency in a reducing atmosphere may lead to the increase of oxygen ion conductivity and decrease of electron conductivity. $SrMn_{0.5}Nb_{0.5}O_{3-\delta}$ might be a candidate for oxygen permeation if the oxygen ion conductivity is reasonably high, which needs further investigation. The material is not ideal for single phase SOFC anode application because the conductivity is insufficient at low p_{O_2} although the chemical stability is acceptable and so could form a component in a composite anode. As the material is p-type, its conductivity will increase under polarisation when used as a SOFC anode due to oxidation. This is an important advantage; however the conductivity is still not quite high enough for efficient electrode operation. The d.c. conductivity of $SrMn_{0.5}Nb_{0.5}O_{3-\delta}$ at low p_{O_2} exhibits a $p_{O_2}^{1/6}$ dependence that is interpreted by a simple defect chemistry model. Similar materials are the subject of further investigation as potential SOFC anodes.

Acknowledgement

We would like to thank EPSRC and NEDO for funding.

References

1 H. L. Tuller, *Solid State Ionics*, 1992, **52**, 135–146.
2 J. T. S. Irvine, D. P. Fagg, J. Labrincha and F. M. B. Marques, *Catal. Today*, 1997, **38**, 467–472.
3 U. Balachandran, B. Ma, P. S. Maiya, R. L. Mieville, J. T. Dusek, J. J. Picciolo, J. Guan, S. E. Dorris and M. L. Liu, *Solid State Ionics*, 1998, **108**, 363–370.
4 S. W. Tao, Q. Y. Wu, Z. L. Zhan and G. Y. Meng, *Solid State Ionics*, 1999, **124**, 53–59.
5 M. Stoukides, *Catal. Rev.*, 2000, **42**, 1–70.
6 K. C. Liang, Y. Du and A. S. Nowick, *Solid State Ionics*, 1994, **69**, 117.
7 A. S. Nowick and Y. Du, *Solid State Ionics*, 1995, **77**, 137.
8 H. G. Bohn, T. Schober, T. Mono and W. Schilling, *Solid State Ionics*, 1999, **117**, 219.
9 A. S. Nowick, Y. Du and K. C. Liang, *Solid State Ionics*, 1999, **125**, 303.
10 R. Glockner, A. Neiman, Y. Larring and T. Norby, *Solid State Ionics*, 1999, **125**, 369–376.
11 A. S. Nowick and K. C. Liang, *Solid State Ionics*, 2000, **129**, 201.
12 K. R. Thampi, A. J. McEvoy and J. Van herle, *J. Electrochem. Soc.*, 1995, **142**, 506–513.
13 A. C. Larson and R. B. Von Dreele, GSAS-Generalised Crystal Structure Analysis System, Los Alamos National Laboratory Report No. LA-UR-86-748, Los Alamos, NM, 1994.
14 S. Fritsch and A. Navrotsky, *J. Am. Ceram. Soc.*, 1996, **79**, 1761–1768.

15 J.-H. Choy, S.-T. Hong and K.-S. Choi, *J. Chem. Soc., Faraday Trans.*, 1996, **92**, 1051–1059.
16 R. D. Shannon and C. T. Prewitt, *Acta Crystallogr., Sect. B*, 1969, **25**, 925–946.
17 A. Kruth and A. R. West, *J. Mater. Chem.*, 2001, **11**, 153–159.
18 H. L. Tuller, *Solid State Ionics*, 1997, **94**, 63–74.
19 J. A. Duffy, *Bonding, Energy & Bands in Inorganic Solids*, Longman Scientific & Technical, Essex, 1990.